Journal of Cosmology (2015), Vol. 24, No. 26, pp 12333-12362

Cratering, Momentum Coupling and Enhancement in Thick Targets

John L. Remo

Departments of Astronomy and Earth and Planetary Sciences, Harvard University,

20 Oxford St. and Harvard-Smithsonian Center for Astrophysics, 60 Garden St.

Cambridge MA, 02138. jremo@cfa.harvard.edu

Abstract: It is analytically shown crater ejecta velocity, momentum coupling, momentum enhancement, and excavation depth profile and mass from impact on thick (non-penetrable) targets are proportional to kinetic high energy density impact velocity, crater energy deposition profile, target, and impactor/target density and vaporization energy. Asymptotic and optimal momentum coupling coefficients are computed and found to be in agreement with experimental values on a variety of planetary and meteoritic target material proxies. A momentum coupling model of the comet Tempel 1 by impact from a projectile shows that momentum enhancement can, for sufficiently high ejecta mass and velocity, dominate the momentum transfer process to a thick target.

Keywords: momentum coupling and enhancement, cratering, ejecta.

1. Introduction

This paper analytically conceptualizes and directly solves one-dimensional high energy density (HED) non-penetrating crater formation, ejecta velocity and optimal momentum transfer, enhancement, and coupling to thick (non-penetrable) targets, e.g. planets, comets, or asteroids, for a high energy density impact velocity, for an arbitrary (depending on projectile materials) crater energy deposition profile and collective mass ejection vaporization energy. The advantage of this direct analytical model approach to an essentially nonlinear multivariable non-equilibrium HED processes is the analysis is quickly and transparently achieved without approximation, within the limits of the proposed models which are themselves approximations. This model explicitly shows interdependences of the key ejection parameters: input velocities, vaporization energies, density, and energy deposition profiles with momentum coupling and enhancement. This putative analytic model which can be used for preliminary calculations is opposed to, but cannot replace, more complex hydrodynamic computer studies that iterate on a complex set of variables which inevitably involves approximations and truncations introducing (often sequestered) errors and may fail in some regimes to provide a clear intuitive sense of the dynamics of the fundamental processes, obscuring the forest for the trees. Another advantage of this analytic model is it can rapidly provide quantitative estimates of crater impact ejection velocities and momentum transfer whereas computer hydrodynamic models provide much greater detail over a range of physical processes. In short, the proposed analytic model is used to, by providing intuitive quantitative guidance, compliment more detailed computer models.

2. Momentum enhancement (ME)

Momentum, p_e, over an area, A, imparted to a target by ejecta, from both the impactor (projectile) and target crater, is found by integrating over an ejecta profile for the relevant crater locations via the integral relationship

$$p_e /A = - \int \rho_c \, v_e \, dz \qquad (1)$$

where ρ_c is the average of the projectile and the ejected crater material densities, v_e is the energy dependent material ejecta velocity opposite in direction to the input velocity, and z is the crater depth. From the impactor density, ρ_i, velocity, v_i , and rear surface ejection velocity, v_e, and rear surface ejecta the enhanced momenta imparted to the target are calculated. Energy initially partitioned into a transient ionization plasma, ~ 1%, is assumed to be adiabatically converted to ablative energy and not taken into account explicitly other than being included in the vaporization energy.

The momentum enhancement (ME) coefficient is defined as the total momentum imparted to the target, p_t, divided by the input (impact) momentum, p_i, such that [1]

$$ME = p_t /p_i \qquad (2)$$

System momentum is conserved where impactor plus ejecta momenta equal the transfer of momentum to the crater target. For ME >1 ejecta is required where [2]

ME = { Impactor momentum - Ejecta momentum }/ Impactor momentum

= Target momentum/ Impactor momentum.

In general

$$ME = 1 - m_e v_e / m_i v_i \qquad (3)$$

m_e and v_e are the collective ejecta mass and velocity ejection vector from a thick (not penetrable) crater; m_i and v_i are the impactor mass and velocity. The ME process
can dominate the momentum transfer process, depending on the mass and velocity of the ejecta. Spallation from the opposite direction of the mass ejecta will reduce the ME.

3. ME and momentum of crater ejecta

The v_e , opposite in direction to the v_i , depend on impactor mechanical energy density, $\varepsilon_i = v_i^2/2$, such that for a constant energy profile with depth [3]

$$v_e = - [2 (\varepsilon_i - \varepsilon_v)]^{1/2} \qquad (4)$$

where ε_v is the collective excavation, decomposition and vaporization energy per kilogram of the impactor and excavated crater. If $\varepsilon_i = ½ \times 10^8$ J/kg (v_i = 10 km/s), $\varepsilon_v = 10^7$ J/kg, v_e = - 8.9 km/s

and for $\varepsilon_v = 10^6$ J/kg, v_e = - 9.7 km/s, exceeding Mars escape velocity at - 5 km/s but not Earth's at - 11.2 km/s. The ME is

$$ME = 1 + [2\,(\varepsilon_i - \varepsilon_v)\,]^{1/2}\, m_e\, / m_i\, v_i \qquad (5)$$

For collective excavation and ejection of crater and impactor mass $M = \rho_c\, V_c + \rho_i\, V_i$

$$ME = 1 + [\,2\,(\,\varepsilon_i - \varepsilon_v)\,]^{1/2}\,((\,\rho_i\, V_i + \rho_c\, V_c\,)/(\rho_i\, V_i\, v_i)) \qquad (6)$$

where ρ_i and V_i are the density and volume of the impactor and ρ_c and V_c are the density and volume of the excavated crater material. For a cylindrical impactor of radius r and length L excavating a cylindrical crater of depth D and radius R

$$ME = 1 + [\,2\,(\,\varepsilon_i - \varepsilon_v)\,]^{1/2}\,[1 + (\rho_c\,/\rho_i)(D/L)\,(R\,/r)^2\,]/v_i \qquad (7)$$

For a uniform projectile L assume a crater penetration $D \approx L\,(\rho_i/\rho_c\,)^{1/3}$. Dividing by v_i and substituting for D/L the ME delivered to the crater target is

$$ME = 1 + [(1 - 2\,\varepsilon_v\,/v_i^2\,)\,]^{1/2}\,[1 + (\rho_c\,/\rho_i)^{2/3}\,(R/r)^2\,] \qquad (8)$$

The ME as a function of v_i^2/ε_v is shown in figure1. In the limit $v_i^2 >> \varepsilon_v$

$$ME = 2 + (\rho_c\,/\rho_i)^{2/3}\,(R/r)^2 \qquad (8a)$$

The collective momentum from the crater ejecta is

$$p_e = m_e v_e = - [2 (\varepsilon_i - \varepsilon_v)]^{1/2} [\pi (R^2 D \rho_c + r^2 L \rho_i)] \quad (9)$$

To convert to mechanical energy fluence, F, ε_i (J/kg) = μ F(J/m^2) where μ (m^2/ kg) = $1/(\rho_c D)$ and $\varepsilon_i = F/ (\rho_c D)$. $F_v = \varepsilon_v / \mu$ is the fluence required to evaporate target material per unit mass. For constant fluence deposition over area A, $F = F_0 >> F_v$ and $R >> r$

$$p_e /A = - [(2 \varepsilon_v) (F_0 \mu/ \varepsilon_v) - 1)]^{1/2} [\pi (R^2 D \rho_c + r^2 L \rho_i)]/\pi R^2 \quad (10)$$

and

$$v_e = - [(2 \varepsilon_v) (F_0 / F_v) - 1)]^{1/2} = - [(2 \varepsilon_v) (\varepsilon_i / \varepsilon_v) - 1)]^{1/2} \quad (11)$$

The impulsive momentum coupling coefficient, C_M, is defined as the momentum (N-s) imparted to a target divided by the impact energy (J) such that

$$C_M = (p_e /A) / F_0 \text{ (s/m)} \quad (12)$$

and

$$C_M = 1.4 \varepsilon_v^{1/2} \rho_c D [F_0/F_v - 1]^{1/2} / F_0 \quad (13)$$

In the asymptotic region $F_0 >> F_v$, the interaction is less efficient and C_M is diminished

$$C_{M\,asym} = 1.4\ \rho_c\ D\ \varepsilon_v^{1/2}\ (F_0/F_v)^{1/2}/F_0 = 1.4\ (\mu\ F_0)^{-1/2}\ (s/m) \qquad (14)$$

Taking the partial derivative of at F_0 for (13), $F_0 = 2\ F_v$ is the maximum impulsive momentum coupling coefficient, $C_{M\,max}$, occurring when ε_v is minimal, converting more energy into momentum transfer, i.e.

$$C_{M\,max} = 1.4\ \rho_c\ D\ \varepsilon_v^{1/2} / F_0 = 0.7\ \rho_c\ D\ (\mu / F_v)^{1/2} = 0.7\ \varepsilon_v^{-1/2}\ (s/m) \qquad (15)$$

For $\varepsilon_v = 4 \times 10^6$ J/kg, $C_{M\,max} = 3.5 \times 10^{-4}$ s/m which agrees with experiments [3].

4. Variable fluence profile

For F = F(z) where z = crater depth, $F = F_0 \exp - (z/D) = F_0 \exp - (z\ \mu\ \rho_i)$.

$$p_e /A = - \int_0^z [(2\ \varepsilon_v)\ (\mu\ F_0\ (\exp - (z/D))/\varepsilon_v - 1)\ ]^{1/2}\ \rho_c\ dz \qquad (16)$$

Integrating (16) as shown in the appendix gives the ejecta momentum per unit area

$$p_e /A = - 2.8\ \varepsilon_v^{1/2}\ \rho_c\ D\ \{\ [F_0/F_v - 1]^{1/2} - Tan^{-1}\ [\ F_0/F_v - 1]^{1/2}\ \} \qquad (17)$$

In the asymptotic limit $(F_0/F_v) >> 1$, the ejecta velocity is

$$v_e = - 2.8 (\varepsilon_v)^{1/2} \{(F_0/F_v)^{1/2} - \pi/2 \} \approx - 2.8 (\mu F_0)^{1/2} \quad (18)$$

Ejection velocity and momentum transfer to craters depend on impact velocity, target volatility, and energy (fluence) absorption profile. The limit $v_e \rightarrow - v_i$ corresponds to reflected incident momentum and exponentially less energy absorbed at greater depths, and has important implications for achievement of escape velocity of impacted material from planetary surfaces and the resulting crater shape.

Momentum coupling for an exponential fluence absorption is

$$C_M = 2.8 \rho_c D \varepsilon_v^{1/2} \{ [F_0/F_v - 1]^{1/2} - \mathrm{Tan}^{-1} [F_0/F_v - 1]^{1/2} \}/ F_0 \quad (19)$$

In the asymptotic region $F_0 >> F_v$,

$$C_{M\,asym} = 2.8 \rho_c D \varepsilon_v^{1/2} \{(F_0/F_v)^{1/2} - \pi/2\}/F_0 \approx 2.8 (\mu F_0)^{-1/2} \text{ (s/m)} \quad (20)$$

Maximum momentum coupling occurs at $F_0 = 6.434 F_v$, and

$$C_{M\,max} = 0.51 \rho_c D \varepsilon_v^{1/2} /F_v = 0.51(\mu F_v)^{-1/2} = 0.51 \varepsilon_v^{-1/2} \text{ (s/m)} \quad (21)$$

indicating a maximum C_M with minimal F_v and maximum excavation depth D and ρ_c .
In general α and β are constants which depend on the material energy deposition profile;

$$C_{M\,asym} = \alpha\, \rho_c\, D\, (\mu/F_0)^{1/2} = \alpha\, (\mu F_0)^{-1/2}\, (s/m) \qquad (22)$$

$$C_{M\,max} = \beta\, \rho_c\, D\, (\mu/F_v)^{1/2} = \beta\, \varepsilon_v^{-1/2}\, (s/m) \qquad (23)$$

For uniform energy deposition $\alpha = 1.4$ and $\beta = 0.7$; for exponential energy deposition $\alpha = 2.8$ and $\beta = 0.51$. As expressed by 14 and 20 the momentum coupling is inversely proportional to the square root of the fluence in the asymptotic regions. Also, as inferred from (15) and (21) objects with volatile compositions, with lower ε_v, such as comets, have greater crater ejection maximum coupling coefficients also modulated by the energy deposition profile constant as shown in (22) and (23).

5. ME and momentum coupling

ME can be expressed in terms of C_M for v_i from ~ 1- 20 km/s [4] by the equation

$$ME = 1 + C_M\, v_i /2 \qquad (24)$$

For the exponential absorption profile

$$ME = 1 + (2\, \varepsilon_v)^{1/2}\, \rho_c\, D\, \{\, [F_0/F_v - 1]^{1/2} - Tan^{-1}\, [\, F_0/F_v - 1]^{1/2}\, \}\, v_i / F_0 \qquad (25)$$

Substituting $v_i = [\, 2\, \mu\, F_0\,]^{1/2}$, then

$$ME = 1 + 2\,(\varepsilon_v\,\mu / F_0)^{1/2}\,\rho_c\,D\,\{\,[F_0/F_v - 1]^{1/2} - Tan^{-1}\,[\,F_0/F_v - 1]^{1/2}\,\} \qquad (26)$$

ME and $C_{M\,max}$ x 10^{-4} are calculated as a function of the penetration factor D/L, $\rho_c/\rho_{i,}$ at v_i = 10 km/s and ε_v = 9 x 10^6 J/kg for uniform and exponential absorption profiles in table 1. Uniform deposition profile calculated ME ≈ 4.0 - 18.5 and $C_{M\,max}$ x 10^{-4} ≈ 6 - 35, agree with comet analog (ice) targets experimental values (table 2) [2] ME ≈ 5.8 - 9.7 and C_M x 10^{-4} ≈ 15 - 25. The exponential profile calculated ME ≈ 3.2 - 13.5 and $C_{M\,max}$ x 10^{-4} ≈ 4 - 25 agree with meteorite analog (rock/iron) targets experimental ME ≈ 1.2 - 4.2 and C_M x 10^{-4} ≈ 3 - 12. Uniform $C_{M\,asym}$ /exponential $C_{M\,asym}$ = $\alpha_{uniform}/\alpha_{exp}$ = 0.5 and uniform $C_{M\,max}$ / exponential $C_{M\,max}$ = $\beta_{uniform}/\beta_{exp}$ =1.4, suggesting larger asymptotic (maximum) ejection momentum from an exponential (uniform) energy deposition profile for ME and C_M. The ME for ice is higher than iron silicates because ice is more volatile.

6. Source craters and ejection velocity

The ratio of maximum momentum coupling of ejecta from a crater with a uniform energy deposition profile is 1.4 times an exponential energy profile because the exponential profile ejects relatively more surface material than the uniform absorption profile. This has important implications for craters as the source of meteoritic ejecta achieving escape velocity and establishing ejecta blankets as a function of energy deposition profile. There is a nexus between impact crater energy deposition profile, shape, material vaporization energy, impact crater debris

momentum coupling, and ejection velocities from planetary surfaces. An important example of this effect is the determination of the (ejection) source crater of the Martian shergottite meteorites where their origin and age are inferred from crater density, ejecta pattern, mineralogy, and shape [5]. Martian meteorites could have undergone and survived intact from impact driven shock metamorphism in excess of the ~ 100's GPa required for tensile fracture (see below) allowing fragments to exceed 5 km/s, required for Mars escape velocity, and thereby be captured by Earth and ultimately discovered. For ε_i = ½ x 10^8 J/kg, v_i = 10 km/s and $\varepsilon_v = 10^7$ J/kg, magnitude v_e = 8.9 km/s > 5 km/s (Mars escape velocity). Impact pressure at 5 km/s, P ~ 75 GPa which is survivable. This analysis is also applicable to shock metamorphism, attenuation, and regolith dispersion [6].

7. Comet Tempel 1 impact enhanced momentum transfer

In 2005 a 370 kg primarily copper projectile impacted the Jupiter family comet Tempel 1 at 10.3 km/s and ejected 15 - 30 x 10^6 kg at ~ 1.5 m/s from the crater excavated on the ~10^{14} kg comet mass [7]. Assuming negligible spallation from the opposite direction of the mass ejecta, from conservation of momentum, the impulsive velocity change of Tempel 1, the ME and δv_{comet} are determined by

$$ME_{comet} = 1 - m_e v_e / m_{cp} v_{cp} \qquad (27)$$

and

$$\delta v_{comet} = (m_{cp}\, v_{cp} - m_e\, v_e)/(m_{comet} + m_{cp} - m_e) \quad (28)$$

where m_{cp} and v_{cp} and m_e and v_e are the mass and velocity of the copper projectile and of the ejecta respectively; m_{comet} is the mass of Tempel 1 assumed to have a density ~ 1. Using above values ME_{comet} = 6.9 -12.8 and δv_{comet} = 0.22 - 0.43 x 10^{-6} m/s, displacing the orbit by 7 – 14 m/y. Ejecta momentum, i.e. ME, dominates momentum transfer to the surviving comet target by a factor ~ 10. Ejecta composed of H_2O ice, talc-like powder silicates, carbonates, amorphous carbon, sulfites and polyaromatic hydrocarbons effected ejection velocities. $C_{M\ comet}$ = 1.24 – 2.48 x 10^{-3} s/m which is expected for an icy comet. The comet ME of 7-14 also in good agreement with experimental values [2].

8. Ejecta particle sizes

The preceding analysis, based on conservation of momentum and energy, does not provide a method to determine ejecta particle size. However, speculating on an order of magnitude estimate on ejecta particle spall thickness, d, ejected from the rear surface of a crater forming impactor is calculated from momentum continuity, d ρ_i v_e**,** used in the equation

$$d\, \rho_i\, v_e \approx T\, L/\, v_i \quad (29)$$

where T is the tensile strength or the bulk modulus. L/v_i ~ the compression time,

$d\ \rho_i\ v_e$ is the ejecta momentum per unit area and $T\ L/v_i$ is the impulse per unit area. For an iron meteorite impact size L = 10 m, density 7,600 kg/m^3, T = 10^9 N/m^2, v_e = 5 km/s and v_i = 10 km/s, d = 2.6 cm. For a stony (olivine) meteorite with density 3,800 kg/m^3, and T = 8 x 10^{10} N/m^2, d = 4.2 m. The mean mass of the initial ejecta particle fragments in the initial spall layer is $m_e = \rho\ \pi\ r^2\ d$ = 621 kg for an iron meteorite and 5 x 10^4 kg for an olvine meteorite cylinder shaped impactor with r = 1m. The impact pressure, P, is

$$P = \rho_i\ v_i^2 \qquad (30)$$

For P = 7.6 x 10^{11} Pa and 3.8 x 10^{11} Pa > T, P is sufficient to overcome tensile strengths of both iron and stony meteorite material suggesting an olivine (stony) impactor will produce a larger size ejecta particles than the iron meteorite. The spall of thickness d from the rear surface generates a reduced internal pressure pulse back into the impactor generating a secondary velocity impulse response, δv, from the spalled surface back to the crater bottom which is again partially reflected where

$$d\ \rho_i\ v_e \approx -\ \delta v\ \rho_i\ (L - d) \qquad (31)$$

Since $\delta v \approx -\ v_e\ d/(L - d)$ and L >> d, $\delta v \rightarrow 0$ (for L/d =100, $\delta v = v_e/100$). The spall process repeats itself as long as pressure on the rear surface of the impactor can overcome T. When the pressure pulse can no longer overcome T there are a series of energy dissipating internal reflections. Higher fragmentation and collision further comminutes and ablates ejected impact fragments.

9. Conclusion

ME, mean ejecta velocity, and momentum coupling occurring during HED crater forming impact are analyzed in closed mathematical form as a function of impact velocity, vaporization energy, densities, and energy deposition profile which in turn effects the crater ejecta velocity, ME, C_M, and excavation profile. There is excellent agreement between experimental and computational values and a uniform crater excavation and energy absorption profile generates higher ME and C_M. This computation suggests higher density lower volatility materials (stone and iron) meteorite and planetary crust and mantle materials have an exponential energy absorption and excavation profile generating lower ME and C_M due to a shallower ejected mass profile. However, asymptotically driven systems favor exponential deposition for higher ejection velocities. Ejecta fragment size and velocity are proportional to the impactor tensile strength. This quantitative analysis can help in intuitively interpreting and understanding HED impact dynamics and cratering problems in general and planetary impact dynamics in particular.

10. Acknowledgement

Very helpful critiques of this manuscript by R. J. Lawrence and P. Hammerling are acknowledged. R. J. Lawrence is also thanked for producing the graphs used in figure 1 and 2.

11. References

1. Lawrence, R. J., Enhanced momentum transfer from hypervelocity particle impacts, *Int. J. Impact Engng, 10,* 337-349, 1990.

2. Remo, J. L. and Furnish, M. D., Radiative and mechanical energy coupling and momentum enhancement to manufactured and planetary materials, in prep 2015.

3. Hammerling, and Remo, J. L., NEO interaction with nuclear radiation, *Acta Astronaut., 36*, 337-346, 1995.

4. Shafer, B. P., Garcia, M. D., Managan, R. A., Remo, J. L., Rosenkilde, C. E., Scammon, R. J., Snell, C. M., and Stellingwerf, R. F., Momentum Coupling to NEOs, in Near Earth Objects: the United Nations International Conference, *Annals of the New York Academy of Science,* vol 822, ed. J. L. Remo, 552-565, 1995.

5. Werner, S. C., Ody, A., and Poulet, F., The source crater of Martian shergottite meteorites, *Science*, *343*, 1343-1346, 2014.

6. Ferriere, L., Koeberl, C., Ivanov, B. A., and Reimold W. U., Shock metamorphism of Bosumtwi impact crater rocks, shock attenuation, and uplift formation, *Science*, *322*, 1678-1681, 2008.

7. A' Hearn, M. F., Belton, M. J. S., Delamere, W. A., Deep impact excavation of Tempel 1, *Science*, 310, 258-264, 2005.

Table 1. ME and $C_{M\,max}$ x 10^{-4} are calculated as function of D/L and ρ_c/ρ_i, impact velocity v_i = 10 km/s, and ε_v = 9 x 10^6 J/kg for uniform and exponential absorption profiles. For a uniform deposition profile calculated ME ≈ 4.0 - 18.5 and $C_{M\,max}$ x 10^{-4} ≈ 6 - 35, agree with comet analog (ice) target experiments (table 2) where ME ≈ 5.8 - 9.7 and C_M x 10^{-4} ≈ 15 – 25 [2]. Exponential profile calculated ME ≈ 3.2 - 13.5 and $C_{M\,max}$ x 10^{-4} ≈ 4 - 25, agree with meteorite analog (rock/iron) targets experimental ME ≈ 1.2 - 4.2 and C_M x 10^{-4} ≈ 3 - 12.

Crater absorption profile	D/L	ρ_c/ρ_i	$C_{M\,max}$ x 10^{-4}	ME
Uniform	5	1.5	18	10.0
	5	1.0	12	7.0
	5	0.5	06	4.0
	10	1.5	35	18.5
	10	1.0	23	12.0
	10	0.5	12	7.0
Exponential	5	1.5	13	7.4
	5	1.0	08	5.2
	5	0.5	04	3.2

10	1.5	25	13.5
10	1.0	17	9.5
10	0.5	09	5.4

Table 2. Experimental values of C_M and ME are listed for targets subjected to an impact projectile velocity ~ 8 km/s and mass = 19.2 x 10^{-6} kg. C_M and ME are larger for the more volatile comet, ice, and snow targets corresponding to uniform energy absorption profiles. Non-volatile targets correspond to the exponential energy absorption profiles.

Target	Density (kg/m^3)	C_M (s/m x 10^{-4})	ME	Crater description
Non-volatile targets				
Scoraceous rock (porous basaltic lava)	1,000	9.6	3.9	Small crater
Andesine basalt (fine grained volcanic rock)	2,900	9.2	3.8	Spall fragments
olivine bomb (magnesium iron silicate)	3,300	11.7	2.9*	Fragmentation
Fe rich olivine	3,500	10.0	4.2	Fragmentation
Fe meteorite Odessa	7,700	2.8	1.2	Small crater

Volatile targets

Comet analog	550	14.6	5.8*	Broad shallow crater
Compacted snow	560	25.0	9.7	Flat crater with substantial material removal
Ice	930	16.6	6.8	Fragmentation

Reference targets

Aerogel	224	11.7	4.8	Deep crater with substantial material removal
Soft wood	-	-	1.0	Complete absorption of slug; inelastic capture

Table 3. Correlation between calculated and experimental values for $C_M \times 10^{-4}$, $C_{M\,max} \times 10^{-4}$, and ME and associated crater shape. Flat craters correspond to uniform energy absorption and steep craters correspond to exponential energy absorption. There is agreement between experimental and calculated values based on the analysis.

Target	$C_M \times 10^{-4}$	$C_{M\,max} \times 10^{-4}$	ME	Crater shape
Calculated @ 10 km/s impact				
Volatile/uniform deposition	X	6.0 - 35	4.0 - 18.5	Broad/shallow
Non - volatile/exp deposition	X	4.0 - 25	3.2 - 13.5	Conical
Experimental @ 8 km/s impact				
Volatile/uniform deposition	14.6 - 25	X	5.8 - 9.7	Broad/shallow
Non - volatile/exp deposition	2.8 - 11.7	X	1.2 – 4.2	Conical

Journal of Cosmology (2015), Vol. 24, No. 26, pp 12333-12362

Appendix A

Integration of the exponentially variable fluence absorption profile

For $F = F(z)$ where z = crater depth, $F = F_0 \exp - (z/D) = F_0 \exp - (z \mu \rho_i)$.

$$p_e /A = - \int_0^z [(2 \varepsilon_v) (F_0 \mu (\exp - (z/D)) / \varepsilon_v - 1)]^{1/2} \rho_c \, dz \qquad (A.1)$$

$$= - (2 \varepsilon_v)^{1/2} \rho_c D \int_0^y (F_0 \mu (\exp - y)) /\varepsilon_v - 1)]^{1/2} \, dy, \qquad (A.2)$$

where $z/D = y$.

Now,

$$p_e /A = - (2 \varepsilon_v)^{1/2} \rho_c D \int_1^{(F0 \mu/ \varepsilon v)^{1/2}} [(F_0 \mu x^{-2} /\varepsilon_v - 1)]^{1/2} \, 2 \, dx /x, \qquad (A.3)$$

where $x^2 = \exp y$, $2 x \, dx = \exp y \, dy$.

$$p_e / A = - 2 (2 \varepsilon_v)^{1/2} \rho_c D \int_1^{(F0\, \mu / \varepsilon v)^{1/2}} [F_0/F_v - x^2)]^{1/2} / x^2] dx \qquad (A.4)$$

Integrating, the specific impulse (momentum per unit area) due to impact ejecta is

$$m_e v_e / A = p_e / A = - 2.8 \varepsilon_v^{1/2} \rho_c D \{ [F_0/F_v - 1]^{1/2} - Tan^{-1} [F_0/F_v - 1]^{1/2} \} \qquad (A.5)$$

In the asymptotic limit $(F_0/F_v) >> 1$, and $Tan^{-1} (F_0/F_v) \approx \pi/2 - (F_v/F_0)$ and

$$v_e = - 2.8 (\varepsilon_v)^{1/2} \{(F_0/F_v)^{1/2} - \pi/2 \} \approx - 2.8 (\mu F_0)^{1/2} \qquad (A.6)$$

Figure 1. ME is plotted as a function of v_i^2/ε_v for three ratios of cylindrical crater to impactor radii squared, $(R/r)^2 = 1$, 4, and 9, and where $k = (\rho_c/\rho_i)(D/L) = 10$. For large values of v_i^2/ε_v ME is asymptotic in $(R/r)^2$.

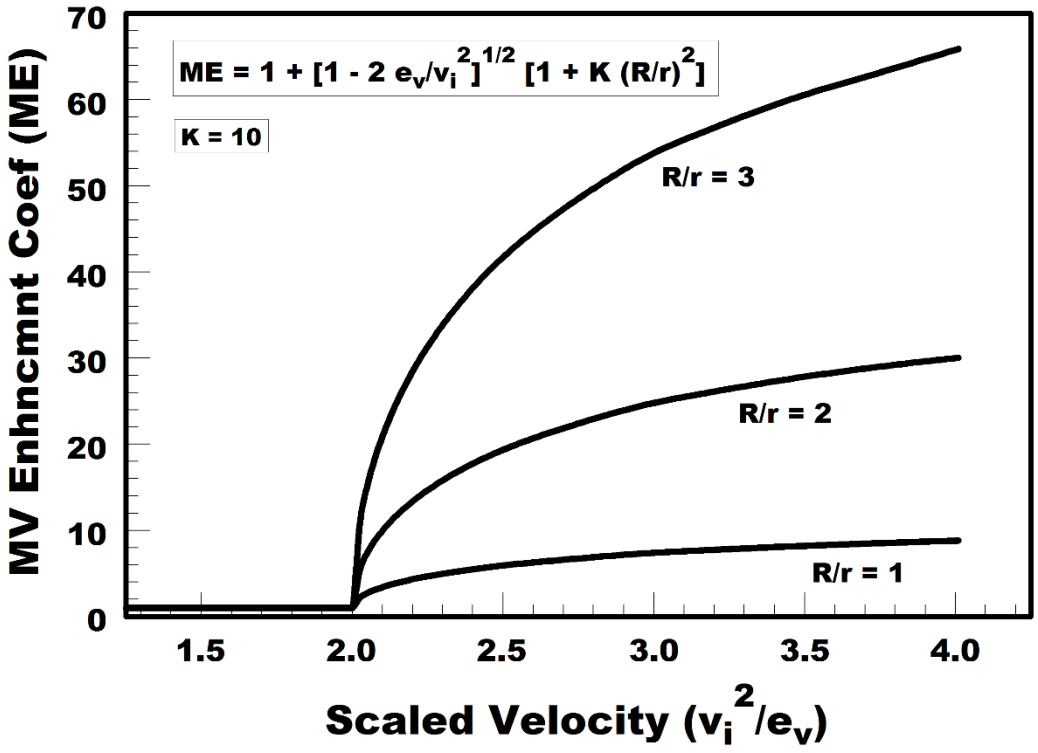

Figure 2. ME is plotted as a function of v_i^2/ε_v for ratios of the crater density, ρ_c, to the impactor density, ρ_i, which is a proportional to ME, suggesting a greater momentum transfer (enhancement) from a relatively lower density impactor whose material provides the majority of the ejecta from the relatively higher density crater which functions as a constraining chamber for the impactor ejecta. When $\rho_c/\rho_i \ll 1$ there is relatively more target excavation and penetration.